TWO BOUNDARY VALUE PROBLEMS FOR THE GINZBURG–LANDAU EQUATION

L. SIROVICH, J.D. RODRIGUEZ
Center for Fluid Mechanics and the Division of Applied Mathematics, Brown University, P.O. Box 1966, Providence, RI 02912, USA

and

B. KNIGHT
Rockefeller University, New York, USA

Two boundary value problems for the Ginzburg–Landau equation are considered. Extensive numerical calculations have been performed in each case, including bifurcation histories, spectral analysis, Poincaré sections and Hausdorff dimension estimates. The approach to the inviscid limit is given detailed treatment. In this case *universal* behavior has been found to exist. Arguments are presented to account for this behavior.

1. Introduction

The Ginzburg–Landau (GL) equation [1] appears as a limit or amplitude equation, in a wide variety of physical applications [2–11]. Instead of considering any specific application, we regard this equation as interesting in its own right, as a general model for the investigation of chaos and low-dimensional attractors. In this paper, the GL equation will be written as

$$G(A) = A_t - q^2(i + c_0)A_{xx} - \rho A$$
$$- (i - \rho)A|A|^2$$
$$= 0. \tag{1.1}$$

Each of the constants q, c_0, ρ are real and positive, and Newell's [12] criterion

$$0 < c_0\rho < 1 \tag{1.2}$$

for instability is assumed. Eq. (1.1) represents a normalized form of the usual representation of the GL equation [13–15].

Eq. (1.1) includes the effects of diffusion, dispersion, linear growth and amplitude-dependent frequency changes. Non-linearity inhibits unbounded growth and solutions remain pointwise bounded (Lagrange stability) [13, 14]. The GL equation describes phenomena in the neighborhood of a critical point of stability, and thus leads to a rich structure of solutions. As a result a variety of numerical experiments have been performed on the GL equation [8, 15–21].

In this paper we consider the Neumann and Dirichlet boundary value problems for eq. (1.1). The former case was treated, in detail, by Keefe [18]. In this instance, only temporal chaos occurs, over the range of parameter space considered. For the Dirichlet problem treated here, the solutions are spatially chaotic as well as temporally.

A main goal of this investigation is the study of complicated dynamics for which the attractor dimension is relatively low. Ghidaglia and Héron [22] have shown that the attractor dimension is finite for the GL equation (see also Doering et al. [23]) and have obtained rigorous estimates for the attractor dimensions. Modulo some fine print, our own informal arguments and numerical estimates for the attractor size show good agreement with their results. Another goal of this study is the approach to *inviscid* flow, i.e. the behavior for small values of q. This we show, analytically and numerically, leads to a universal form for the energy spectrum.

In the following paper [24] (henceforth known as II), we use the calculations described in this paper as baseline data, to obtain equivalent low-dimensional dynamical systems.

2. Problem definition

The GL equation (1.1) is normalized so that the domain of interest is

$$0 \le x \le \pi. \tag{2.1}$$

In our investigation q is the bifurcation parameter, and can be related to a wavenumber. Decreases in q correspond to increases in the domain size.

As stated in section 1, two boundary value problems will be considered. The first of these is specified by homogeneous Neumann conditions,

$$\frac{\partial}{\partial x} A(0) = \frac{\partial}{\partial x} A(\pi) = 0. \tag{2.2}$$

The second problem is specified by homogeneous Dirichlet conditions,

$$A(0) = A(\pi) = 0. \tag{2.3}$$

Since the GL operator respects odd and even symmetry, we may solve (1.1), under the boundary conditions (2.2), by expanding the amplitude A in

the complete set $\{\cos nx\}$,

$$A = \sum_{n=0} A_n(t) \cos nx. \tag{2.4}$$

Similarly under (2.3), (1.1) can be solved in the form

$$A = \sum_{n=1} A_n(t) \sin nx. \tag{2.5}$$

(In the actual numerical calculations a pseudo spectral method is employed [25].) We mention in passing that (1.1) is invariant under multiplication by a constant lying on the unit circle, i.e.

$$G(A) = 0 \Rightarrow G(e^{ic}A) = 0 \tag{2.6}$$

for any real constant c.

3. Chaotic attractors

One facet of our study is the investigation of the chaotic attractor. The term attractor has the usual meaning of being a set to which almost all nearby trajectories tend, and a trajectory once on the attractor remains there for all time. The term chaotic also has the usual sense, namely that nearby trajectories on the attractor diverge exponentially. (But only for finite time since the attractors in question are compact.) For q^{-2} large enough the solutions are chaotic. The GL equation is dissipative and as a result the actual dimension of the attractor can be expected to be significantly smaller than the space in which the dynamics takes place.

To estimate the attractor dimension we use the Kaplan–Yorke formula [26]

$$d_L = N - \frac{1}{\lambda_{N+1}} \sum_k^N \lambda_k. \tag{3.1}$$

This requires the determination of the Lyapunov exponents, λ_k. N in (3.1) refers to the largest integer for which the sum is non-negative. Meth-

ods for the determination of the Lyapunov exponents are well known [27–29]. The essential step in these approaches lies in carrying the linearized or variational equations along in the integration of the non-linear equations. For the GL equation the linearized equation is

$$\delta G = \partial_t \delta A - q^2 (i + c_0)(\delta A)_{xx} - \rho \, \delta A$$
$$- (i - \rho)(2\bar{A}_0 \delta A + A_0 \delta \bar{A})$$
$$= 0, \tag{3.2}$$

where A_0 denotes the *reference* solution to the GL equation (1.1) and δA, the variation. To find M Lyapunov exponents, we must simultaneously integrate M replicas of (3.2) (with appropriate initial data) in addition to (1.1).

Keefe [18] instead integrates $M + 1$ replicas of the GL equation, each with slightly differing initial data. Keefe also adopted this approach in his investigation of turbulent plane Poiseuille flow [30]. Deissler [31], MacGiolla-Mhuris [32] and Grappin and Leorat [33] have used the approach presented in the previous paragraph in considering the Navier–Stokes equations.

It is implicit to this method that the reference trajectory visits almost all of the chaotic attractor. A customary additional condition is that the attractor must be non-decomposable. While this makes obvious good sense it should be noted that there are at least three disjoint attractors in the present situation. The two problems posed in section 2 may be regarded as 2π-periodic solutions which are evolving on the entire real line. Since the GL equation respects odd and even symmetry, even or odd initial data evolve in time in what might be termed even and odd subspaces. Thus the Neumann problem will have a chaotic attractor in the even subspace and the Dirichlet problem a chaotic attractor in the odd subspace. Although we do not consider such a case, there will also be a chaotic attractor for cases without such symmetries. These three attractors have no cross-talk, i.e. they are disjoint. The set of circumstances just described poses no problem for us. For example in computing the attractor of the Dirichlet case we are assuming that the reference trajectory visits all of just this attractor and this is the essential requirement.

As a last remark along these lines, it is important to note that each of the problems give rise to two zero Lyapunov exponents. One zero exponent corresponds to the fact that $A(t - t_0)$ satisfies the GL equation for all t_0 (or $\delta A = \partial_t A_0$ satisfies (3.2)). The other zero exponent follows from the invariance (2.6) (or $\delta A = i A_0$ satisfies (3.2)). It therefore follows from (3.1) that any chaotic solution must have dimension greater than three.

4. Neumann problem

For the Neumann problem in the range

$$0.6 \le q \le 1.33 \tag{4.1}$$

a sequence of behavior is uncovered. (Here and in the following we take $\rho = c_0 = 1/4$ in the numerical solution of (1.1).) This is summarized in fig. 1 [18]. At $q \approx 1.33$ the spatially independent Stokes solution, e^{it}, bifurcates to a limit cycle with spatial structure. The early stage can be described analytically through linear theory [13] and the subsequent transition to two-torus motion follows from Floquet theory [34].

If (3.1) is used to calculate the attractor dimension, we obtain the plot shown in fig. 2 for the first window of chaos shown in fig. 1. A maximum Lyapunov dimension, d_L, is achieved at $q \approx 0.95$ with [18]

$$d_L \approx 3.047. \tag{4.2}$$

The temporal energy spectrum at this value is broad band [15, 18]. In fig. 3 we show the time evolution of A for $0 \le x \le \pi$ at $q = 0.95$. Thus while the motion associated with A is temporally chaotic, its spatial dependence is regular. The spatial energy spectrum shows few active Fourier components [18].
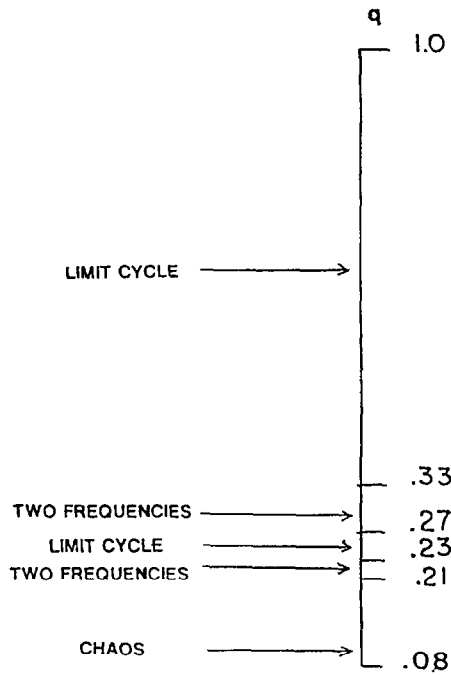
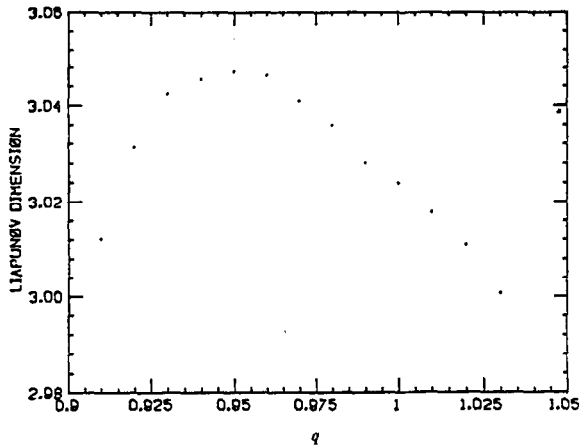Fig. 1. Bifurcation sequence, Neumann problem.

Fig. 2. Lyapunov dimension, Neumann problem.

Fig. 3. Time history (20 time units) Neumann problem; (a) real part, (b) imaginary part.

5. Dirichlet problem

There is a marked difference in the behavior of solutions for Dirichlet boundary conditions. By fixing the boundary condition to be the homogeneous Dirichlet conditions, we consider a more constrained class of flows, and thus instability and its consequence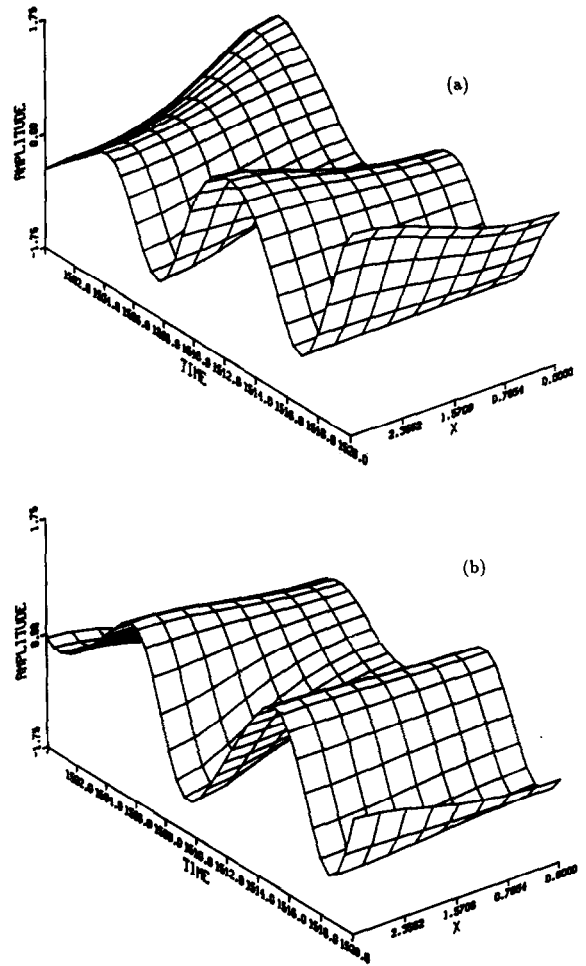s are deferred. On the other hand, one can expect a more pronounced boundary layer in this case. A summary of behavior, over the range considered here, is shown in fig. 4. This problem has not been previously discussed in the literature and certain features of fig. 4 merit discussion.

For relatively large values of q the homogeneous solution

$$A = 0 \tag{5.1}$$
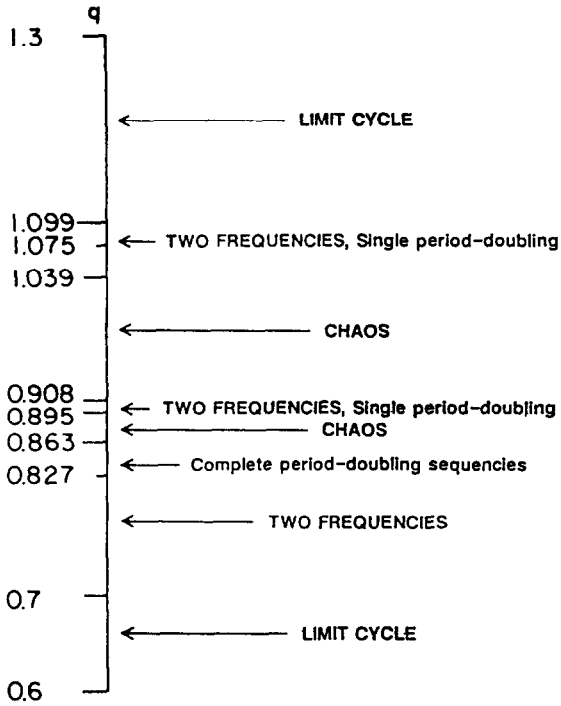
is stable. In particular, if we consider solutions

Fig. 4. Bifurcation, Dirichlet problem.

having the form

$$A \propto e^{\sigma t} \sin nx \qquad (5.2)$$

in the linearized equation form of (1.1) we obtain

$$\sigma_r = \rho - n^2 q^2 c_0 \qquad (5.3)$$

for the real part of the complex growth rate. Thus the solution is unstable for

$$q_0^2 = \rho / c_0 > n^2 q^2 \qquad (5.4)$$

and $n = 1$ is the most unstable harmonic. Since the number of unstable modes is equal to the dimension of the unstable manifold, this is given by the integer part of $1/q$ (recall that $\rho = c_0 = 0.25$). This fixes a lower bound on the attractor dimension.

At $q = 1$ the zero solution undergoes a Hopf bifurcation and the solution is linearly unstable to the first Fourier harmonic. Non-linear interactions

produce all odd harmonics, and a stable limit cycle results. As may be verified directly, limit cycle solutions can be written in factorable form,

$$A = \phi(x) e^{i\Omega t}, \qquad (5.5)$$

where ϕ satisfies [34]

$$i\Omega\phi - q^2(i + c_0)\phi_{xx} - \rho\phi - (i - \rho)\phi|\phi|^2 = 0. \qquad (5.6)$$

If we write

$$q^2 = q_0^2 - \epsilon^2 \qquad (5.7)$$

with ϵ^2 small, a straightforward perturbation analysis yields

$$\phi \sim \frac{4c_0}{\rho_0}\epsilon \sin x = 4\epsilon \sin x \qquad (5.8)$$

and

$$\Omega \sim -q_0^2 + \left(1 + \frac{c_0}{\rho_0}\right)\epsilon^2 = -1 + 2\epsilon^2, \qquad (5.9)$$

for $\rho = c_0 = 0.25$. Thus the frequency is initially negative and then increases as q^2 decreases. Fig. 5 displays the exact non-linear dispersion relation, gotten by solving (5.6) under periodic boundary conditions. A time stationary solution appears at $q = 0.70148$. (Note that this is well approximated
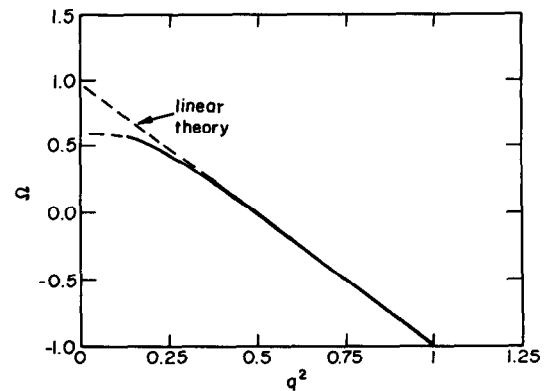

Fig. 5. Dispersion relation, limit cycle frequency, Ω, versus q^2.

by the linear theory (5.9), indicated by a dashed line, which gives $q = 1/2 \approx 0.707$.) A feature of the limit cycles in the range $0.34 < q < 1$, is that although the second Fourier harmonic is unstable for $q < 0.5$, the solution possesses no even harmonics. If a set of initial data having only even harmonics is assumed, parity conditions show that a limit cycle solution in only even harmonics emerges. However, such a solution is unstable to perturbations by odd harmonics, and a limit cycle solution results which possesses no even harmonics.

This phenomenon is the result of the invariance of the subspaces spanned by the even and odd modes. This in turn is due to the cubic non-linearity. The first mode is unstable, and even if an initial condition is taken with no first mode present, any odd mode will produce a first mode by non-linear interaction. The most unstable even mode is the second, nevertheless, its growth is still slower than that of the first mode. The first mode initially grows rapidly and quickly reaches a bound. Inspection of the equations shows that at that point, the non-linear interactions in the even modal equations produce a negative forcing, this damps out the even modes, and leaves a solution with purely odd modes. At $q = 0.34$ the limit cycle solution becomes unstable and an odd harmonic two-torus motion appears. This persists until $q = 0.27$, when a limit cycle solution reappears. The reemergence of limit cycle behavior is accompa-

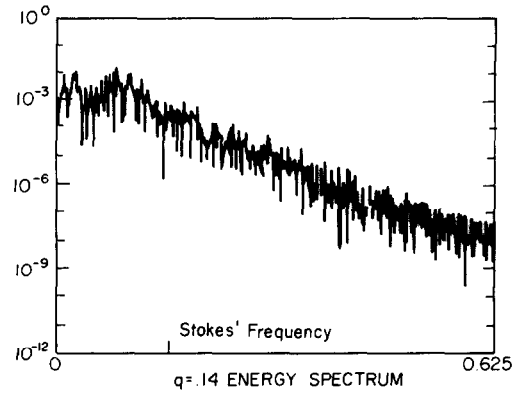
Fig. 7. Energy spectrum, Dirichlet problem, $q = 0.14$.

nied by the appearance of both even and odd harmonics in the solution.

As q is decreased further a brief window of two-torus motion again appears at $q = 0.23$, and at $q = 0.21$ chaos appears. Unlike the Neumann problem the chaos manifests itself in a continuous band with no *relaminarization*. A plot of the attractor dimension based on the Kaplan–Yorke formula is shown in fig. 6, for $0.08 < q < 0.21$, and as can be seen no local maximum occurs. (For small values of q, the Neumann also exhibits pronounced chaos [35].)

At the nominal reference value of $q = 0.14$ the Lyapunov dimension is 9.1. Fig. 7 shows the energy spectrum and fig. 8 the averaged wavenumber spectrum at this same value of q. This last figure
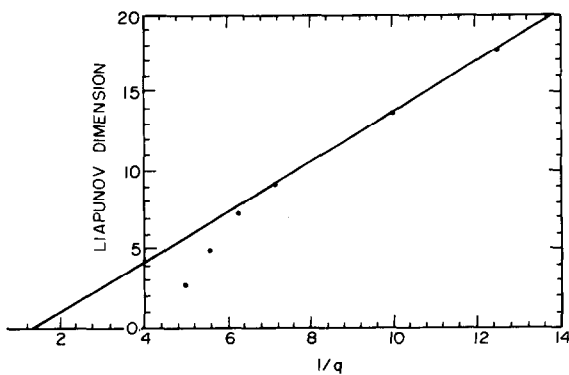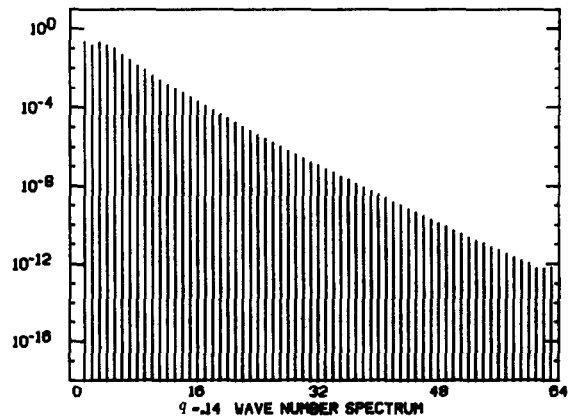

Fig. 6. Lyapunov dimension, Dirichlet problem.

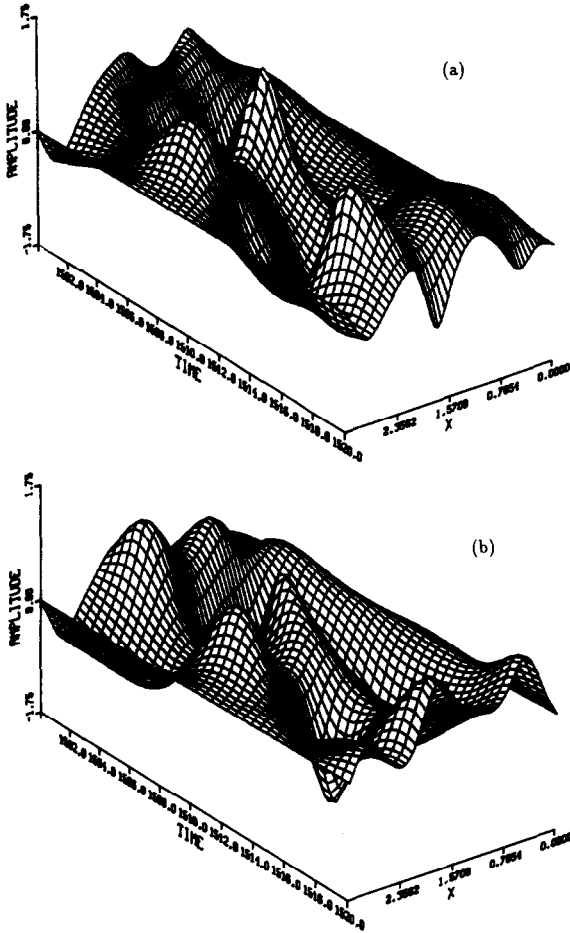Fig. 8. Wavenumber spectrum, Dirichlet problem, $q = 0.14$.

Fig. 9. Time history (20 time units) Dirichlet problem; (a) real part, (b) imaginary part.

shows that a *broad* spectrum of wavenumbers enters in the *flow* at this value of q. This is further underlined by the time evolution of the solution as shown in fig. 9.

6. Nearly inviscid flows

As $q \downarrow 0$ the *viscous* scale decreases in magnitude and numerical calculations of a solution becomes more demanding. In this section we use numerical experiments as a basis for predicting general features under this limit. While most of the arguments are general, the discussion will be

carried out within the framework of the Dirichlet problem. Under the transformation

$$y = x/q, \tag{6.1}$$

(1.1) becomes

$$A_t - (i + c_0) A_{yy} - \rho A - (i - \rho)|A|^2 A = 0 \tag{6.2}$$

and (2.1),

$$A(0) = A(L = \pi/q) = 0. \tag{6.3}$$

The limit in this format is one in which the *box* becomes infinite.

6.1. Lyapunov dimension

Fig. 6 implies that the Lyapunov dimension becomes linear in q^{-1} as $q \downarrow 0$. This can be arrived at by an informal argument. If in (1.1), we apply the limit $q \downarrow 0$ we obtain

$$A_t - \rho A - (i - \rho) A |A|^2 = 0, \tag{6.4}$$

which is a singular limit. Eq. (6.4) is easily integrated, and its solutions tend, asymptotically, to the Stokes solution. Up to an arbitrary phase this is given by

$$A = e^{it}. \tag{6.5}$$

This does not satisfy the boundary condition (2.3) and therefore implies the existence of a boundary layer, of size

$$\delta \approx q(1 + c_0^2)^{1/4}. \tag{6.6}$$

This is not the smallest scale in the problem, but rather is an estimate for the correlation length. The smallest scale, i.e. the smallest that we must resolve, is given by

$$\hat{\delta} = q c_0^{1/2}. \tag{6.7}$$

This is the dissipative length scale, or what in

turbulence is referred to as the Kolmogorov microscale. Thus the number of scales, or degrees of freedom, which must be resolved is given by

$$d \approx L/\hat{\delta} = \pi/qc_0^{1/2}. \qquad (6.8)$$

(This also serves as the basis for determining the number of *degrees of freedom* needed in the numerical integration.) If, as is often supposed, the Lyapunov dimension and the number of degrees of freedom are proportional, then (6.8) confirms that asymptotically d_L is proportional to $1/q$, as is implied by fig. 6.

6.2. Spatial power spectrum

Therefore, from the lower bound given by the unstable manifold estimate and (6.8) we have

$$1/q < d < \pi/c_0^{1/2}q. \qquad (6.9)$$

From fig. 6 we see that the numerical value of the slope is roughly 1.7.

Ghadaglia and Héron [25] have obtained rigorous upper and lower bounds for the attractor dimension of the GL equation. Since they consider the more general, and less restrictive, problem of periodic boundary conditions their estimates, while $\mathcal{O}(1/q)$, are less sharp. (Actually the estimates of Ghadaglia and Héron contain undetermined constants which one supposes are $\mathcal{O}(1)$.)

In view of the complex diffusivity in (6.2), the scale δ (6.6) is the measure of a nominal oscillation and therefore estimates the correlation length. Since $c_0 = \mathcal{O}(1)$ above boundary layer analysis implies that the dissipative scale, $\hat{\delta}$, and the correlation length, δ, are of the same order. This will have an interesting consequence in regard to the spatial power spectrum. As we have already noted, the attractor dimension is $\mathcal{O}(1/q)$. This suggests that in plotting the spectrum we should use nq as the abscissa. Alternatively, if we view the problem as one in which the box size increases indefinitely,

then nq represents the *wavenumber* in this limit. Fig. 10 exhibits the spatial power spectrum, plotted in this style, for a sequence of values of q down to $q = 2 \times 10^{-2}$. As q decreases we see that two ranges emerge; first a flat, energy bearing range, which we refer to as the integral range, then at an index of $\mathcal{O}(1/q)$ this changes fairly abruptly to a dissipative range, which appears to have a near exponential falloff. Thus the number of active modes is well estimated by (6.9). The continuous curve in fig. 10 is the spectrum for $q = 0.06$. It is seen to be a template for all the spectra, thus implying a universal spectrum. In the remainder of this section we present arguments which imply the presence of *universal* features as $q \downarrow 0$.

6.3. A universal spectrum

We first consider the integral range. Fig. 11 displays a typical instantaneous snapshot of the solution for $q = 0.02$, at which spatial chaos is present. Consider the Fourier coefficients in (2.5)

$$A_n = \frac{2}{\pi} \int_0^\pi A(x,t) \sin nx \, dx. \qquad (6.10)$$

Fig. 11 implies that for $q \downarrow 0$, the interval of integration can be decomposed into many sub-intervals of length large compared with the correlation length, (6.6), and small compared to π. Since the spatial behavior is chaotic, the sum over the subintervals, which approximates (6.10), is a random walk on the complex plane and from the central limit theorem, the time series for each A_n is Gaussian distributed. This argument only requires that

$$n \ll 1/q, \qquad (6.11)$$

since it is being supposed that $\sin nx$ is piecewise constant in each of the subintervals. It follows that the same statistics will be valid for all n satisfying condition (6.11).

The above argument predicts that $\langle |A_n|^2 \rangle$ is roughly constant for index n satisfying (6.11).
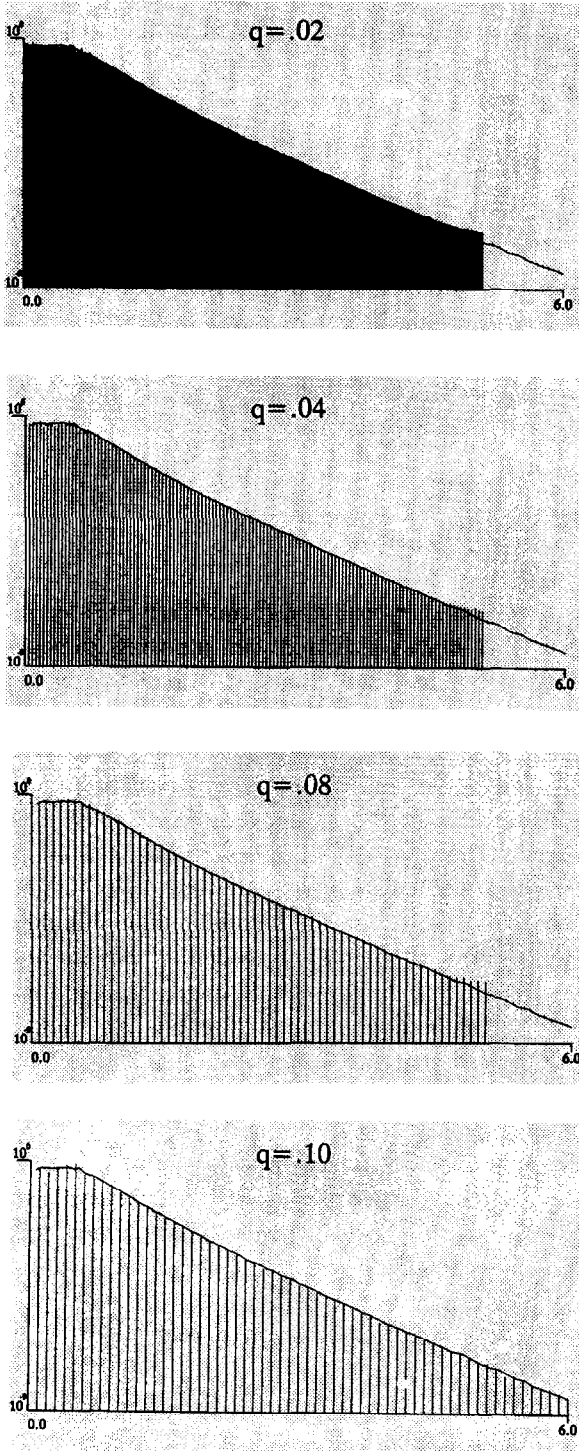
q=.02

q=.04

q=.08

q=.10

Fig. 10. Wavenumber spectra plotted in universal form, i.e. $|A_n|^2/q$ versus nq for $q = 0.02, 0.04, 0.08, 0.10$. The continuous curve is the wavenumber spectrum at $q = 0.06$.
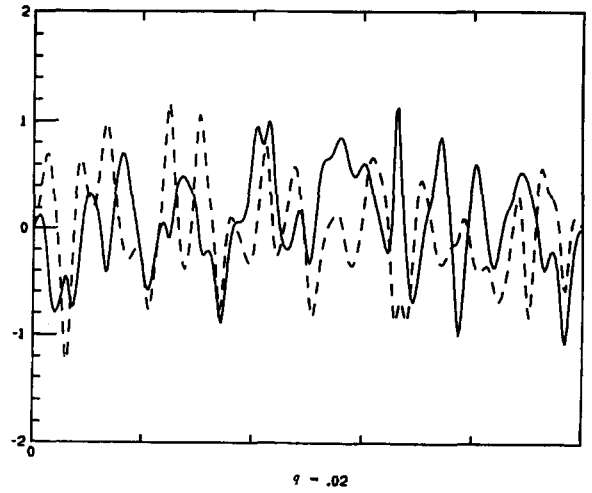

$q = .02$

Fig. 11. Instantaneous snapshot of A for $q = 0.02$. Continuous and dashed curves represent the real and imaginary parts, respectively.

While the results displayed in fig. 8 cannot be regarded as confirming this assertion (in this instance $1/q \approx 7$) the sequence shown in fig. 10 clearly indicates the trend toward

$$\langle |A_n|^2 \rangle = \epsilon(q), \tag{6.12}$$

where, as indicated, the average depends on q.

To calculate the constant which appears in (6.12) we observe that

$$\langle \|A\|^2 \rangle = \left\langle \frac{1}{\pi} \int_0^\pi |A|^2 \, \mathrm{d}x \right\rangle$$

$$= \tfrac{1}{2} \sum_n \langle |A_n|^2 \rangle. \tag{6.13}$$

From the above arguments and the numerical evidence we can write

$$\langle \|A\|^2 \rangle \approx \tfrac{1}{2} \sum_{n=1}^{\mathcal{O}(1/q)} \langle |A_n|^2 \rangle. \tag{6.14}$$

Table 1
Some values for eq. (6.12) for different values of q.

q	0.01	0.02	0.04	0.08	0.10
$\langle \|A\|^2 \rangle$	0.42	0.412	0.404	0.425	0.41

In table 1 we list some of the values of (6.12) which we have calculated.

For $q \downarrow 0$ almost all the energy resides in the modes for which (6.11) holds. For these, the diffusion term in (1.1) is small and the GL equation is approximated by (6.4). If $\rho \downarrow 0$, this equation is Hamiltonian with

$$H = |A|^4/4 = (X^2 + Y^2)^2/4, \tag{6.15}$$

where we have written

$$A = X + iY. \tag{6.16}$$

(Although $\rho = 1/4$ is not small we adopt this as the approximation.) Next we argue that as a result of the diffusion nearby positions in x are only weakly coupled so that the probability of finding a state A is given by

$$P(A) = \frac{e^{-\beta H}}{Z} = \frac{e^{-\beta(X^2 + Y^2)^2/4}}{Z}, \tag{6.17}$$

where β is the reciprocal *temperature*, and the *partition function* is given by

$$Z = \pi^{3/2}/\beta^{1/2}. \tag{6.18}$$

If we denote averages with respect to (6.16) by square brackets then the condition that H be statically stationary is

$$[dH/dt] = 2\rho[|A|^4 - |A|^6] = 0, \tag{6.19}$$

which after a straightforward calculation yields

$$\beta = 16/\pi. \tag{6.20}$$

From this we obtain

$$1/2 = [|A|^2] \approx \langle \|A\|^2 \rangle, \tag{6.21}$$

which in view of the size of ρ is in reasonable agreement with the values shown in table 1.

We may also undertake the calculation for the dissipative range of the spatial power spectrum. This is done in the appendix.

7. Further comments

Two boundary value problems for the GL equation have been considered. On imposing homogeneous boundary conditions we force a *boundary layer* on the solution. While this delays instability, and ultimately chaos, it is seen to also produce a richer chaotic state. The degree of chaos is well illustrated in fig. 11, an instantaneous snapshot of the *flow* for $q = 0.02$. In the case of the Neumann problem the flow goes through windows of relaminarization while for the Dirichlet case this does not occur. Keefe [35] has considered the Neumann case down to relatively small values of q and has not found relaminarization. He has also found indications that the Lyapunov dimension of the attractor does show systemic growth as $q \downarrow 0$. It is likely therefore that the arguments given in section 6 apply to the Neumann problem once q is sufficiently small, since the effect of the boundaries should be of little consequence roughly one boundary thickness removed from them. A similar remark applies to the periodic GL equation without spatial odd and even symmetry.

Appendix

Since boundary effects should become insignificant in the interior of the flow we can consider the related problem of periodic solutions to (1.1),

$$A = \sum_n a_n e^{inx} \tag{A.1}$$

with $-\pi < x < \pi$. The Fourier components of (A.1) satisfy

$$\frac{\partial a_n}{\partial t} + n^2 q^2 (i + c_0) a_n - \rho a_n - (i - \rho) \frac{1}{2\pi} \int_{-\pi}^{\pi} e^{-inx} |A|^2 A \, dx = 0. \tag{A.2}$$

It is clear from inspection that in the limit q fixed and $|n| \uparrow \infty$ the second and fourth term dominate. From this it follows that

$$a_n \approx \frac{i - \rho}{n^2 q^2 (i + c_0)} \mathscr{E}_n, \tag{A.3}$$

where

$$\mathscr{E}_n = \frac{1}{2\pi} \int_{-\pi}^{\pi} e^{-inx} |A|^2 A \, dx = \sum_{\substack{m, q, p \\ m+p-q=n}} a_m a_p \bar{a}_q. \tag{A.4}$$

For $|n| \uparrow \infty$, the dissipative modes and those in the integral ranges become well separated. Then, since the dominant terms lie in the integral range I (the flat portion of the spectra in fig. 10), (A.4) is approximated by

$$\mathscr{E}_n \sim \sum_{m, p \in I} a_m a_p \bar{a}_{m+p-n} + z \sum_{m, p \in I} a_m \bar{a}_p a_{p+n-m}. \tag{A.5}$$

On forming the ensemble average, denoted by angular brackets, of $|a_n|^2$ we obtain

$$\begin{aligned} \langle |a_n|^2 \rangle = \epsilon \Bigg(& \sum_{m, p, m', p' \in I} \langle \bar{a}_{m+p-n} a_{m'+p'-n} \rangle \langle a_m a_p \bar{a}_{m'} \bar{a}_{p'} \rangle \\ & + 4 \sum_{m, p, m', p'} \langle a_{n+m-p} \bar{a}_{n+m'-p'} \rangle \langle a_p \bar{a}_m \bar{a}_{p'} a_{m'} \rangle \\ & + 2 \sum_{m, p, m', p'} \left(\langle \bar{a}_{m+p-n} \bar{a}_{n+m'-p'} \rangle \langle a_m a_p \bar{a}_{p'} a_{m'} \rangle + \text{c.c.} \right) \Bigg), \end{aligned} \tag{A.6}$$

where

$$\epsilon = (1 + \rho^2) / \left[n^4 q^4 (1 + c_0^2) \right]. \tag{A.7}$$

In writing (A.6) we have assumed that the dissipative modes and those in the integral are sufficiently separated ($|n| \uparrow \infty$) so that they are incoherent, and that the ensemble averages can be put in the factored

form that is shown. Since solutions of the GL equation are invariant under multiplication by $e^{i\beta}$ (β real) it follows that the last term vanishes under the ensemble average.

Next it is plausible to assume that the modes in the dissipative range are themselves incoherent. From this it follows that

$$\langle |a_n|^2 \rangle = \epsilon \left(\sum_{\substack{m,\,p,\,m',\,p' \in I \\ m+p=m'+p'}} \langle |a_{n-(m+p)}|^2 \rangle \langle a_m a_p \bar{a}_{m'} \bar{a}_{p'} \rangle + 4 \sum_{m,\,p,\,m',\,p'} \langle |a_{n+m-p}|^2 \rangle \langle a_p \bar{a}_m \bar{a}_{p'} a_{m'} \rangle \right),$$

(A.8)

where we have used

$$\langle |a_{n-s}|^2 \rangle = \langle |a_{s-n}|^2 \rangle.$$

(A.9)

We set

$$f_n = \langle |a_n|^2 \rangle$$

(A.10)

and express (A.8) as a convolution

$$f_n = \epsilon \sum_s f_{n-s} R_s.$$

(A.11)

After some manipulation of terms, the convolution kernel R_s can be shown to take on the form

$$R_s = \langle | \sum_{m \in I} a_m a_{s-m} |^2 \rangle + 4 \langle | \sum_{m \in I} a_m \bar{a}_{m-s} |^2 \rangle.$$

(A.12)

Generally speaking each term of (A.12) has the form of an autocorrelation. While we have no rigorous estimates for these quantities, simplified models give an exponential falloff for R_s.

In order to model the behavior of the dissipative spectrum we replace the integral range by a delta function and simply take

$$R_s = \alpha^{|s|},$$

(A.13)

where $0 < \alpha < 1$. The equation to be solved is therefore

$$f_n - \epsilon \sum_s f_{n-s} \alpha^{|s|} = \delta_{n0}.$$

(A.14)

(The summation can be extended to the full line, since by assumption this only contributes negligibly.)

Except for the fact that ϵ is a function of n, (A.14) is easily solved. Since ϵ, (A.7), is algebraic it is slowly varying on the scale of R_s. Therefore in the spirit of WKB theory we solve (A.14) by first assuming ϵ to be

constant. This yields for $n > 0$

$$f_n = \frac{\epsilon}{z^n} \frac{\alpha^{-1} - \alpha}{\sqrt{b^2 - 4}}, \tag{A.15}$$

where

$$b = b(n) = \alpha + \alpha^{-1} - \epsilon(n)(\alpha^{-1} - \alpha) \tag{A.16}$$

and

$$z = z(n) = \tfrac{1}{2}\left[b(n) + \sqrt{b^2(n) - 4} \right], \tag{A.17}$$

where the slow dependence on n has been made explicit. With WKB theory in mind we now revise (A.15) to read

$$f_n = \frac{\epsilon(n)(\alpha^{-1} - \alpha)}{\sqrt{b^2(n) - 4}} \frac{1}{\prod_{k=1}^{n} z(k)}. \tag{A.18}$$

Some simple numerical experiments verify that (A.18) is extremely accurate for ϵ small.

The shape of the curve f_n versus n closely resembles the dissipative range seen in fig. 10. In particular the upward concavity seen in this figure arises in (A.18) from the *amplitude* term

$$\epsilon(n) \propto e^{-\ln(nq)^4}. \tag{A.19}$$

References

[1] V.L. Ginzburg and L.D. Landau, Zh. Eksp. Teor. Fiz. 20 (1950).

[2] A.C. Newell and J.A. Whitehead, Finite bandwidth, finite amplitude convection, J. Fluid Mech. 38 (1969) 279.

[3] S. Kogelman and R.C. DiPrima, Phys. Fluids 13 (1970) 1.

[4] K. Stewartson and J.T. Stuart, J. Fluid Mech. 48 (1971) 529.

[5] L.M. Hocking and K. Stewartson and J.T. Stuart, J. Fluid Mech. 51 (1972) 705–735.

[6] D.J. Benney and G.J. Roskes, Stud. Appl. Math. 48 (1969) 337–385.

[7] H. Hasimoto and H. Ono, J. Phys. Soc. Japan 33 (1972) 805.

[8] Y. Kuramoto, Prog. Theor. Phys. Suppl. 64 (1978) 346.

[9] Y. Kuramoto and T. Yamada, Prog. Theor. Phys. 56 (1976) 670.

[10] Y. Kuramoto and S. Koga, Phys. Lett. A 92 (1982) 1.

[11] M. Pavlik and G. Rowlands, J. Phys. C 8 (1975) 1189.

[12] A.C. Newell, in: Nonlinear Wave Motion, ed. A.C. Newell (Am. Math. Soc., Providence, RI, 1974).

[13] P.K. Newton and L. Sirovich, Instabilities of the Ginzburg–Landau equation: periodic solutions, Quart. Appl. Math. 44 (1986) 49–58.

[14] L. Sirovich and P.K. Newton, in: Stability of Time Dependent and Spatially Varying Flows, eds. D.L. Dwoyer and M.Y. Hussaini (Springer, Berlin, 1986).

[15] L. Sirovich and J.D. Rodriguez, Coherent structures and chaos: a model problem, Phys. Lett A 120 (1987) 211–214.

[16] H.T. Moon, P. Huerre and L.G. Redekopp, Three-frequency motion and chaos in the Ginzburg–Landau equation, Phys. Rev. Lett. 49 (1982) 7.

[17] H.T. Moon, P. Huerre and L.G. Redekopp, Transitions to chaos in the Ginzburg–Landau equation, Physica D 7 (1983) 135–150.

[18] L. Keefe, Dynamics of perturbed wavetrain solutions to the Ginzburg–Landau equation, Stud. Appl. Math. 73 (1985) 91.

[19] C.S. Bretherton and E.A. Spiegel, Intermittency through modulational instability, Phys. Lett. A 96 (1983) 152–156.

[20] R.J. Deissler, J. Stat. Phys. 40 (1985) 371–395.

[21] K. Nozaki and N. Bekki, Phys. Rev. Lett. 51 (1983) 24.

[22] J.M. Ghidaglia and B. Héron, Dimension of the attractors

associated to the Ginzburg–Landau partial differential equation, Physica D 28 (1987) 282–304.

[23] C. Doering, J.D. Gibbon, D. Holm and B. Nicolaenko, Low dimension behavior in the complex Ginzburg–Landau equation, Contemp. Math. AMS, to appear.

[24] J.D. Rodriguez and L. Sirovich, Low-dimensional dynamics for the complex Ginzburg–Landau equation, Physica D 43 (1990) 77–86.

[25] D. Canuto, M.Y. Hussaini, A. Quarteroni and T.A. Zang, Spectral Methods in Fluid Mechanics (Springer, Berlin, 1988).

[26] J. Kaplan and J. Yorke, in: Functional Differential Equations and Approximation of Fixed Points, eds. H.O. Peitgen and H.O. Walther (Springer, Berlin, 1979).

[27] G. Bennetin, L. Galgani, A. Giorgilli and J.-M. Strelcyn, Lyapunov characteristic exponents for smooth dynamical systems. A method for computing all of them, Meccanica 15 (1980) 9–30.

[28] I. Shimada and T. Nagashirmi, A numerical approach to ergodic problem of dissipative dynamical systems, Prog. Theor. Phys. 61 (1979) 1605.

[29] A. Wolf, J.B. Swift, H.L. Swinney and J.A. Vastano, Deterministic Lyapunov exponents from a time series, Physica D 16 (1985) 285–317.

[30] L. Keefe, Bull. Am. Phys. Soc. Ser. II 32 (1979) 2026.

[31] R.J. Deissler, Phys. Fluids 29 (1986) 1453.

[32] N. MacGiolla-Mhuris, Quart. Appl. Math., to appear.

[33] R. Grappin and J. Leorat, Phys. Rev. Lett. 59 (1987) 1100–1103.

[34] L. Sirovich and P.K. Newton, Periodic solutions of the Ginzburg–Landau equation, Physica D 21 (1986) 115–125.

[35] L. Keefe, private communication.